Journal of Marine Science and Technology

Volume 21 | Issue 3 Article 8

THE VARIATION OF FLEXURAL RIGIDITY FOR POST-TENSIONED PRESTRESSED CONCRETE BEAMS

Ta-Heng Wang
Department of Harbor and River Engineering, National Taiwan Ocean University, Keelung, Taiwan, R.O.C., big-sky@umail.hinet.net

Ran Huang
Department of Harbor and River Engineering, National Taiwan Ocean University, Keelung, Taiwan, R.O.C.

Tz-Wei Wang
Registered Civil and Structure Engineer of R.O.C

Journal of Marine Science and Technology, Vol. 21, No. 3, pp. 300-308 (2013)
DOI: 10.6119/JMST-012-0508-2

THE VARIATION OF FLEXURAL RIGIDITY FOR POST-TENSIONED PRESTRESSED CONCRETE BEAMS

Ta-Heng Wang[1], Ran Huang[1], and Tz-Wei Wang[2]

Key words: natural frequency, prestressed concrete beam, softening.

ABSTRACT

The natural frequency of axial-loaded concrete beam decreases with increasing applied compressive force, and the natural frequency of tensioned cable increases with increasing tensile force. However, the variation of natural frequency of prestressed concrete beam (PCB) consisting of concrete and cable has rarely been discussed based on both |the rigorous mathematic model and experimental results. In this study, a testing program was conducted and Rayleigh's method was used to derive an approximate equation for computing natural frequency. The results indicate that (1) the natural frequency decreases with increasing prestressing force for PCB with eccentric parabolic tendon, but it is no change for PCB with eccentric straight tendon, (2) the proposed equation was proved to be an adequate method for estimating first mode natural frequency in vertical direction, and (3) a modified computed method for effective moment of inertia of PCB was also proposed.

I. INTRODUCTION

From the previous literatures [10, 12], the natural frequency ω_n in vertical direction for a simply supported beam subjected to an axial compressive force is computed as

$$\omega_n = (\frac{\pi}{l})^2 (\frac{EI}{m})^{1/2} (n^4 - n^2 \frac{P}{P_{cri}})^{1/2} \quad (1)$$

$$\omega_n^2 = (\frac{n\pi}{l})^4 (\frac{EI}{m}) - (\frac{n\pi}{l})^2 (\frac{P}{m}) \quad (1a)$$

And for a cable stretched between two fixed ends with a distance l, the natural frequency ω_n of the cable is computed as

$$\omega_n = \frac{n}{2l} (\frac{T}{m})^{1/2} \quad (2)$$

where l is the length of span, EI is flexural rigidity, m is mass per unit length, P is compressive force, P_{cri} is Euler buckling load, T is the tensile force in the cable, and n is the order number of vibration modes. The above-mentioned equations illustrate that the vertical natural frequency of concrete beam will decrease with increasing axial compressive force, and conversely the natural frequency of tensioned cable will increase with increasing tensile force. But only a few researches discussed the variation of the natural frequency for prestressed concrete beams (PCB)s which are composed of concrete beam and prestressing cable.

Kanaka and Venkatesawa [9] formulated the natural frequency using Rayleigh-Ritz method for simply supported beam subjected to axial compressive force. The axial compressive force have significant effect on the lower mode vibration. In 1994, Saiidi [11] conducted a field bridge test and |a laboratory test. The natural frequencies and static vertical deflection were measured and it was found both natural frequency and effective rigidity decreased with decreasing axial compressive force. However, the testing results contradicted the theoretical prediction. He explained that the decrease of the natural frequency or effective rigidity could be due to the development of micro-crack resulting from prestress losses. His explanation induced 3 discussions. The discussions from Deak [5] and Jain [7] pointed out that an internal prestressing force would not reduce the natural frequency of PCB, but no experimental data or mathematical model were proposed to verify their hypothesis. The other discussion from Dall'Asta and Dezi [3] indicated that Eq. (1a) was proper to predict the natural frequency for concrete beam subjected to external force, but not for PCB. They proposed a modified Eq. (3) which was obtained by subtracting compressive stress from elastic modulus (E) to predict ω_n for PCB with axial prestressing force. Where P is prestressing force and A is the cross section area of concrete beam.

Paper submitted 03/09/12; revised 04/30/12; accepted 05/08/12. Authors for correspondence: Ta-Heng Wang (e-mail: big-sky@umail.hinet.net).
[1] Department of Harbor and River Engineering, National Taiwan Ocean University, Keelung, Taiwan, R.O.C.
[2] Registered Civil and Structure Engineer of R.O.C.

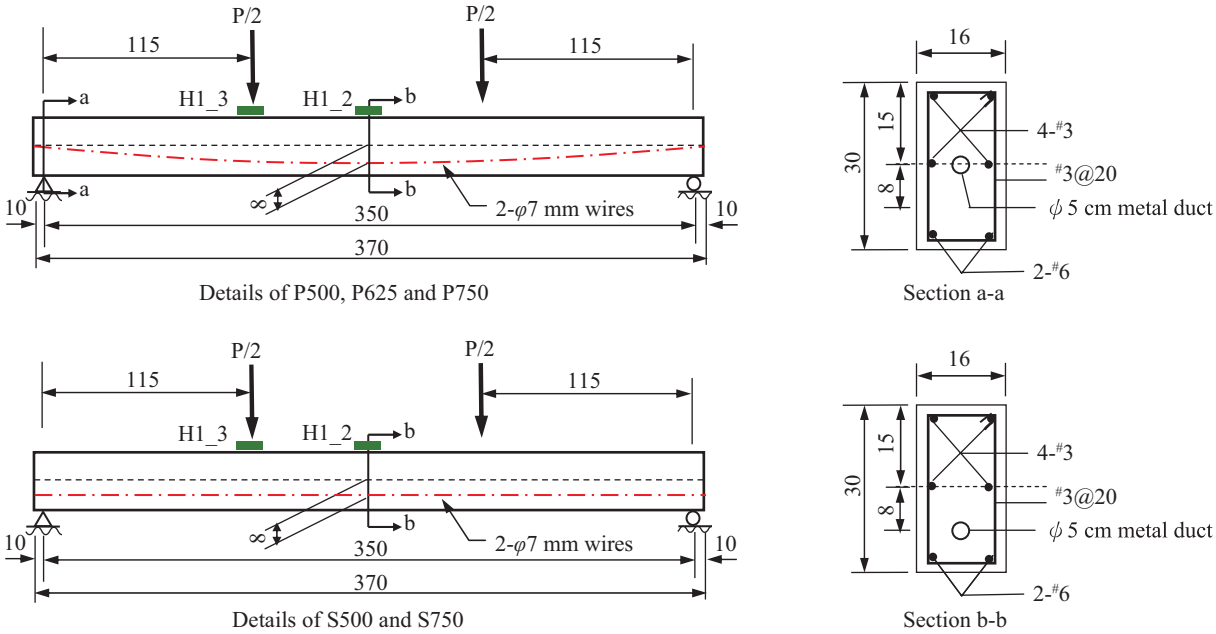

Fig. 1. Details of specimens.

$$\omega_n^2 = (\frac{n\pi}{l})^4(\frac{I}{m})(E-\frac{P}{A})-(\frac{n\pi}{l})^2(\frac{P}{m}) \quad (3)$$

Prior to 1994, the studies of natural frequency variation for PCB were focused on PCB with straight cable but without eccentricity. Until 1996, Dall'Asta and Leoni [4] used kinematic model to derive a complicated mathematical formulation for PCB with internal frictionless eccentricity curve cables. It was found that by increasing prestressing force, the natural frequency would decrease which was about equivalent to 10%~20% loss of elastic modulus. In 2006, Hamed and Frostig [6] derived a governing equation of motion for the dynamic behavior of PCB with bonded and unbonded tendons by using the variation principle of virtual work and Hamilton's principle. His conclusion was opposite to some previous research results. He pointed out that the prestressing forces didn't affect the dynamic behavior of PCB with bonded tendon and the natural frequency could be determined by linear elastic beam theory. But for PCB with un-bonded tendon, a modified model was proposed. In 2009, Breccolotti *et al.* [2] established a structural model which could be solved using commercial software ABAQUS 6.7. Breccolotti *et al.* [2] and Hamed [6] obtained similar conclusions. For PCB with unbonded tendon, the compression softening phenomenon was prominent, but not for PCB with bonded tendon.

From the aforementioned discussion, further study was needed to clarify the variation of natural frequency or rigidity for PCB due to internal axial stress. In this study, the natural frequencies before prestressing, after prestressing without grouting, and after grouting were measured for five post-tensioned PCB specimens. The P-Δ relationships were also monitored to evaluate the variation of flexural rigidity for bonded PCB. In addition, analytical results obtained from Rayleigh's method were compared to the testing results.

II. EXPERIMENTAL PROGRAMS

1. Specimens

Five post-tensioned prestressed concrete beams were cast and tested. All the beams were designed with same geometric dimensions and steel reinforcement. For minimizing prestressing losses at transfer, BBRV wire post-tensioning system was selected. Two $\varphi 7$ mm-coated stress-relieved wires which meeting the requirements of ASTM A421 were placed in a $\varphi 5$ cm metal duct as prestressing tendon in each beam. The metal duct were grouted after prestressing. Three beams with parabolic curve tendon were stressed to 0.50, 0.625 and 0.75 f_{pu}, (equivalent to 31.4, 39.3 and 47.1 KN prestress force was applied) and were designated as P500, P625 and P750, respectively. The parabolic curve of tendon was designed with eccentricity e = 0 at both ends and e = 8 cm at center. Other two beams with straight tendon placed as a constant eccentricity of 8 cm were streessed to 0.50 and 0.75 f_{pu} (equivalent to 31.4, and 47.1 KN prestress force was applied) and were designated as S500 and S750, respectively. The average compressive strength of concrete was 25.48 MPa. Details of testing specimens are shown in Fig. 1.

2. Frequency Measurement

Piezotronics Model 086D20 impact hammer kits which including impact hammer, accelerometers, dynamic signal analyzer and displayer as shown in Fig. 2. were used to measure the frequencies of each specimen at three stages:

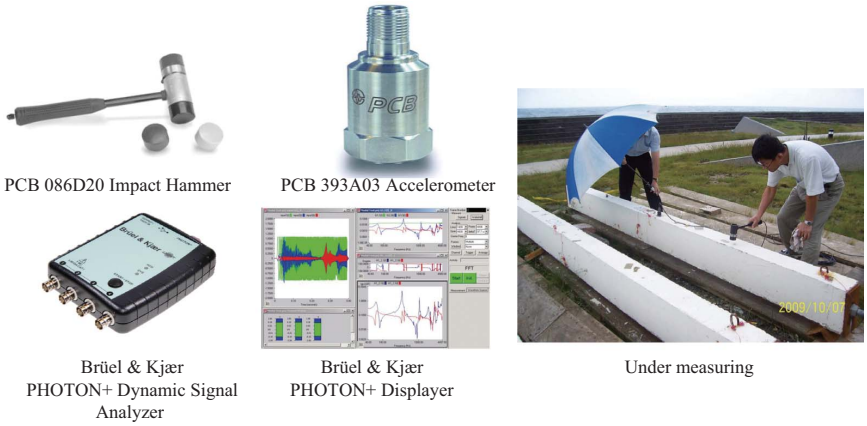

Fig. 2. Impact hammer kits and specimens under testing.

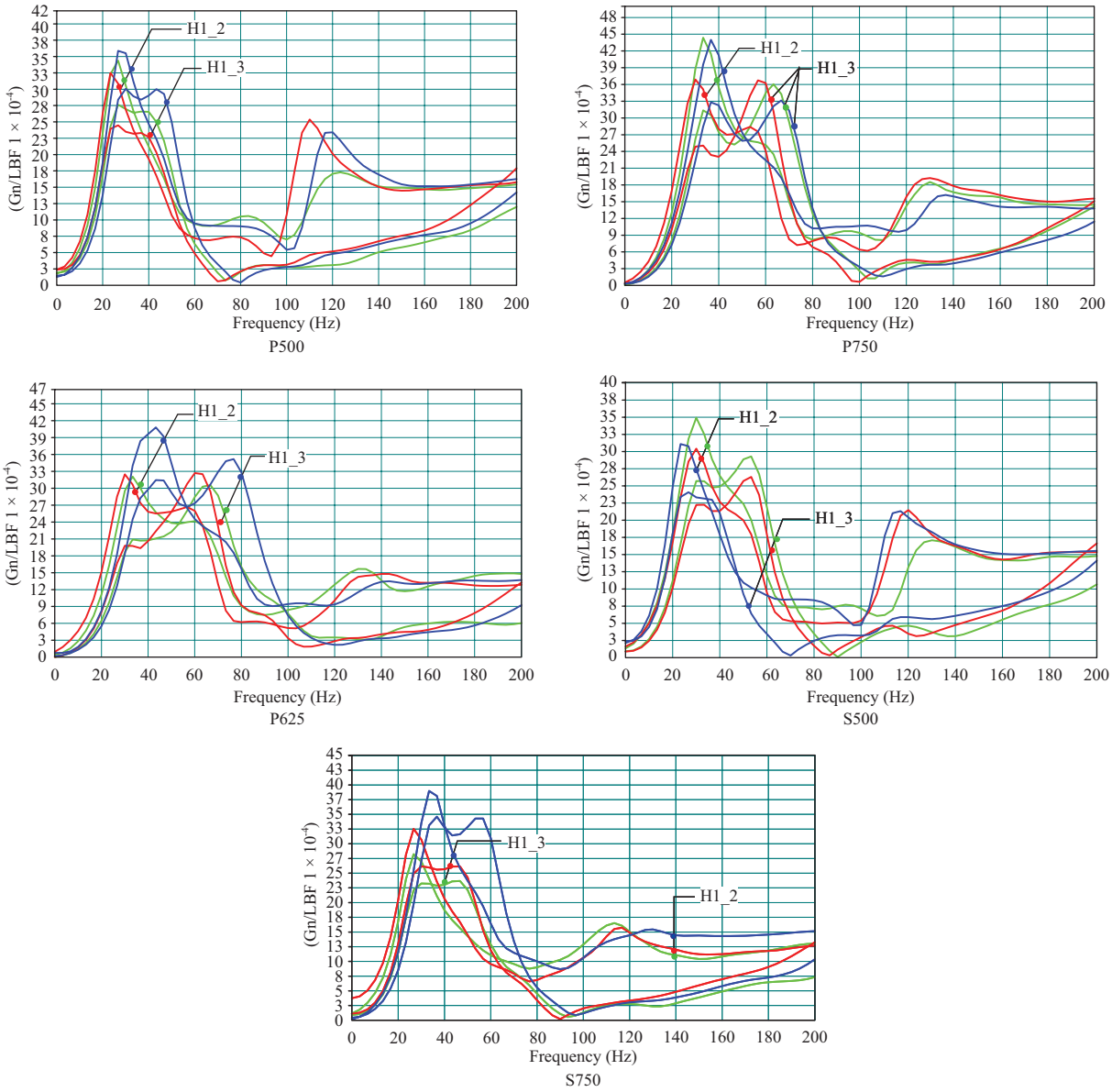

Fig. 3. Natural frequency spectra of specimens.

Table 1. The first two measured natural frequencies in vertical direction of specimens.

Specimen Designation	Prestressing Force P_s (KN)	1st. mode (Hz)			2nd. mode (Hz)		
		ω_{b1}	ω_{p1}	ω_{g1}	ω_{b2}	ω_{p2}	ω_{g2}
P500	31.39	27.00	26.20	27.00	123.50	110.00	116.70
P625	39.24	33.80	32.00	43.50	132.20	130.00	140.00
P750	47.09	36.00	33.00	36.50	130.50	130.00	135.60
S500	31.39	33.00	33.00	23.30	131.00	120.00	116.70
S750	47.09	30.30	30.30	33.30	113.30	116.70	129.50

Fig. 4. P-Δ loading test.

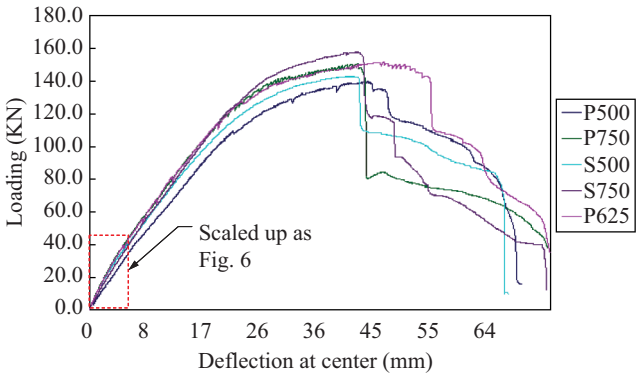

Fig. 5. Loading – deflection diagram.

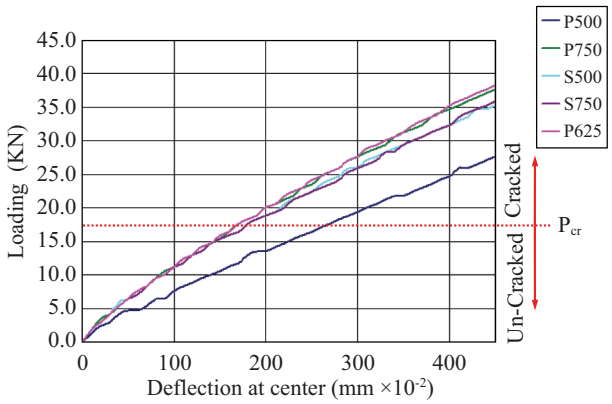

Fig. 6. Scaled up part of Fig. 5.

before prestressing (simulating RC beams), prestressed before grouting (simulating unbonded PCB) and after grouting (simulating bonded PCB). Based on SIMO (single-input, multiple-output) approach, two accelerometers (H1_2 and H1_3) were attached on the top surface at 1/2 and 1/3 spans of beam as shown in Fig. 1 for measuring vertical vibration for each input excitation. The recorded natural frequency spectra are illustrated in Fig. 3 in which each stage is marked as green (1st. stage), red (2nd. stage) and blue (3rd. stage) color, respectively. The natural frequencies of first two modes were obtained from the peak values and listed in Table 1. Where ω_{b1}, ω_{p1}, and ω_{g1} represents the first mode of natural frequency for PCB before applying prestress, prestressed and without grouting and prestressed with grouting, respectively, similarly ω_{b2}, ω_{p2}, and ω_{g2} is the second mode of natural frequency for PCB at various stages.

3. Load-Deflection Test

Load-deflection tests were conducted in the laboratory to estimate the flexural rigidity of specimens. The test set-up as shown in Fig. 4, each specimen was equally loaded at two points 115 cm away from supports. Three electronic gages connected to a data acquisition system were arranged under two loading points and middle point. Deflection was recorded at each 0.6 KN increment until failure. The load-deflection curves for five specimens are illustrated in Fig. 5 and partial curves are magnified as in Fig. 6 for estimating flexural rigidity of the uncracked specimen.

For predicting the immediate deflection after cracking, the effective moment of inertia, I_e, was suggested as Eq. (4) by ACI [1].

$$I_e = \left(\frac{M_{cr}}{M_a}\right)^3 I_g + \left[1-\left(\frac{M_{cr}}{M_a}\right)^3\right] I_{cr} \tag{4}$$

Where $M_{cr} = \dfrac{f_r I_g}{y_t}$, f_r is rupture modulus of concrete which is taken as $0.6\sqrt{f_c'}$ for normal weight concrete, I_g is moment of inertia of gross section, y_t is distance from central axis of gross section to tension face, and M_a is maximum moment in member due to loading at stage deflection is computed.

Following Notes on ACI 318-95 [8], the moment of inertia of a cracked beam with tension reinforcement and prestressing

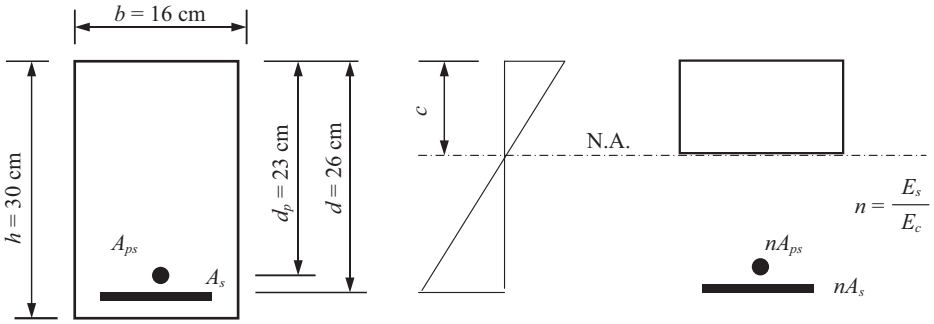

Fig. 7. Cracked Transformed Section of PCB.

tendon I_{cr} is computed in the following manner.

Taking moment of areas about neutral axis in Fig. 7

$$b\times c\times\frac{c}{2}=nA_s(d-c)+nA_{ps}(d_p-c) \tag{5}$$

The moment of inertia of cracked section about neutral axis can be expressed as

$$I_{cr}=\frac{bc^3}{3}+nA_s(d-c)^2+nA_{ps}(d_p-c)^2 \tag{6}$$

All of 5 specimens are designed with the same dimensions and amount of non-presstressed and prestressed steel which are b = 16 cm, d = 26 cm, d_p = 23 cm, E_s = 28,200 MPa, E_c = 23,726 MPa, $n = E_s/E_c$ = 8.48, A_{ps} = 0.772 cm^2, A_s = 5.7 cm^2.

Solving Eq. (5)
c = 10.27 cm.
Substituting c and above data into Eq. (6)
I_{cr} = 18,791 cm^4.

For each specimen, the immediate deflection curve (black line) computed with E_c and I_e which is obtained by substituteing I_{cr} into Eq. (4) is plotted together with testing load-deflection curve as shown in Fig. 8.

III. THEORETICALS

Rayleigh's method is one of the methods for determining an approximate fundamental natural frequency. Since the system of simply support PCB is conservative, based on Rayleigh's principle, the maximum kinetic energy $T_{max.}$ is equal to the maximum potential energy $V_{max.}$. By equating $T_{max.}$ to $V_{max.}$, the fundamental natural frequency ω can be founded.

The kinetic energy of PCB can be expressed as

$$T=\frac{1}{2}\int_0^l \dot{y}^2 dm=\frac{1}{2}\int_0^l \dot{y}^2\rho(x)dx \tag{7}$$

Where dm is mass of the element, $\rho(x)$ is mass per unit length, and y is harmonic moving equation assumed as $y = w(x)\cos\omega t$, then $\dot{y}(t)=-\omega w(x)\sin\omega t$. The term $w(x)$ is assumed as vertical deformed shape function of beam. Then the maximum kinetic energy can be expressed as

$$T_{max}=\frac{1}{2}\int_0^l(\dot{y}(t)_{\max})^2\rho(x)dx=\frac{\omega^2}{2}\int_0^l\rho(x)[w(x)]^2dx \tag{8}$$

By disregarding the work done by shear forces, the potential energy of the deformed beam can be expressed as

$$V=\frac{1}{2}\int_0^l Md\theta \tag{9}$$

Where M is the bending moment expressed by $M = EI\frac{\partial^2 y}{\partial x^2} = EI\frac{\partial^2 w}{\partial x^2}\cos\omega t$, θ is the slope of deformed beam, then $\theta=\frac{\partial y}{\partial x}=\frac{\partial w}{\partial x}\cos\omega t$ and $d\theta=\frac{\partial^2 w}{\partial x^2}\cos\omega t$. By substituting M and $d\theta$ into Eq. (9), then

$$V=\frac{1}{2}\int_0^l(EI\frac{\partial^2 w}{\partial x^2})(\frac{\partial^2 w}{\partial x^2})\cos^2\omega t dx$$

$$=\frac{1}{2}\int_0^l EI(\frac{\partial^2 w}{\partial x^2})^2\cos^2\omega t dx \tag{10}$$

The maximum value of V is

$$V_{max.}=\frac{1}{2}\int_0^l EI(\frac{\partial^2 w}{\partial x^2})^2 dx \tag{11}$$

Let $T_{max.} = V_{max.}$, the fundamental natural frequency ω can be founded

$$\omega^2=\frac{\frac{1}{2}\int_0^l EI(\frac{\partial^2 w}{\partial x^2})^2 dx}{\frac{1}{2}\int_0^l\rho(x)(w(x))^2dx} \tag{12}$$

For simply supported non-prestressed concrete beams, The shape function in vertical direction $w(x)$ is assumed as Eq. (13),

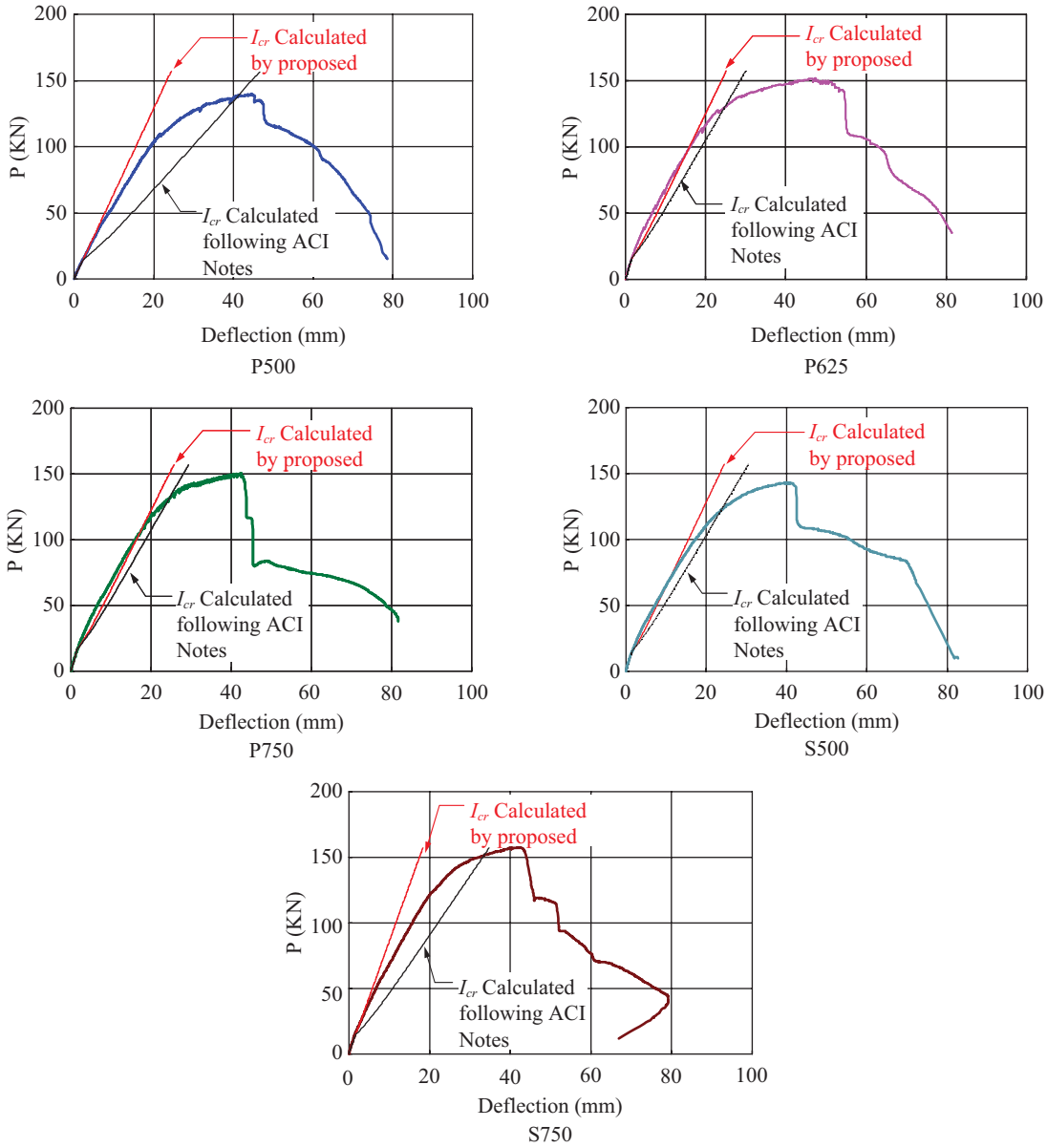

Fig. 8. Comparison of immediate deflections computed following ACI Notes with proposed.

$$w(x) = K(l^3x - 2lx^3 + x^4) \tag{13}$$

where $K = \dfrac{\gamma_0}{24EI}$, γ_0 is unit weight of beam and x is the section position distance from the original point.

By substituting Eq. (13) into Eq. (12), the first mode of natural frequency ω_1 can be found and expressed as Eq. (14). Comparing Eq. (14) with Eq. (1) which use n = 1 and P = 0, the ω_1 computed by Eq. (14) is very close to the value computed by Eq. (1).

$$\omega_1^2 = \left(\frac{V_{max}}{T_{max}}\right) = \frac{3024EI}{31ml^4} \approx \frac{\pi^4 EI}{ml^4} \tag{14}$$

For beams with parabolic pre-stressing tendons, an additional moments dM_p induced by pre-stressing forces at x as shown in Fig. 9 exists in the specified section. By force equilibrium,

$$dM_p + (P_s + dP_s)(e(x) + de)\cos(\alpha(x) + d\alpha)$$

$$-P_s e(x)\cos\alpha(x) - P_s \sin\alpha(x)dx = 0$$

$$dM_p = P_s e(x)\alpha(x)d\alpha - P_s de + P_s\alpha(x)dx - e(x)dP_s \tag{15}$$

where P_s is prestressing force, dP_s is the change of prestressing force which will increase in one side and decrease in the other side for beams with symmetrical tendon and prestress at

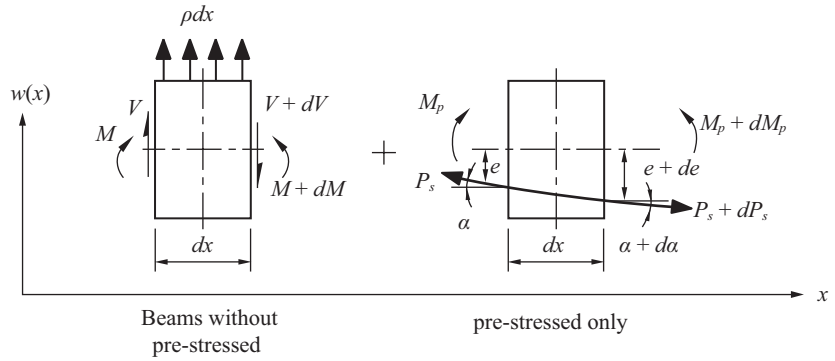

Fig. 9. An element of PCB with prestressed tendon.

both ends. Therefore the effects of dP_s will be vanished each other in the process of integration and can be neglected.

The term $e(x)$ is the eccentricity of tendon at x. For beams with parabolic tendon (P500, P625 and P750), the profile of parabolic tendons as shown in Fig. 1 is:

$$e(x) = \frac{4e_0}{l^2}(x^2 - lx) = C(x^2 - lx) \tag{16}$$

where $C = \frac{4e_0}{l^2}$

$$\frac{de}{dx} = \tan\alpha = C(2x - l) \approx \sin\alpha \approx \alpha \tag{17}$$

where α is curvature of tendon profile

$$\therefore de = \alpha dx \tag{18}$$

$$\frac{d\alpha}{dx} = \frac{d^2e}{dx^2} = 2C$$

$$\therefore d\alpha = 2Cdx \tag{19}$$

Then Eq. (13) can be derived as $dM_p = 2C^3P_s(x^2 - lx)(2x - l)dx$, and the additional moment M_x at x is shown as Eq. (20)

$$M_x \int_0^x dM_p = P_sC^3(x^4 - 2lx^3 + l^2x^2) \tag{20}$$

Then the maximum potential energy $V_{max.}$ can be shown as Eq. (21). The first term in right side of equal sign in Eq. (21) is potential energy for beams without pre-stress, and the second term is additional potential energy due to pre-stress.

$$V_{max} = \frac{1}{2}\int M(x)\,d\theta$$

$$= \frac{1}{2}\int_0^l EI[w''(x)]^2\,dx + \frac{1}{2}\int_0^l M_x w''(x)\,dx$$

$$= \frac{12}{5}EIK^2l^5 - \frac{3}{70}P_sC^3Kl^7 \tag{21}$$

The maximum kinetic energy $T_{max.}$ for PCB with parabolic tendons are un-changed. Based on Rayleigh's principle, the first natural frequencies for PCB with parabolic tendons can be shown as Eq. (22).

$$\omega_1^2 = \left(\frac{V_{max}}{T_{max}}\right) = \left(\frac{3024 - 1296P_sC^3l^2/\gamma_0}{31ml^4}\right)EI \tag{22}$$

For beams (S500 and S750) with straight prestressing tendon, the profile $e(x)$ as shown in Eq. (16) is constant. Then Eq. (11) dM is zero and the first mode of natural frequencies should be similar to natural frequencies of reinforced concrete beams.

IV. RESULTS AND DISCUSSION

1. Variation of Flexural Rigidity

To understand the variation of flexural rigidities for PCB, the first step is to determine the initial flexural rigidity $(E_cI_0)_i$ of each specimen before prestressing. There are three initial flexural rigidities $(E_cI_0)_{iACI}$, $(E_cI_0)_{i\omega}$ and $(E_cI_0)_{iP\Delta}$ computed by three approaches listed in Table 2. Where I_0 is moment of inertia of net cross section before grouting, $(E_cI_0)_{iACI}$ is the product of E_c computed following ACI 8.5.1 and I_0, $(E_cI_0)_{i\omega}$ is computed by measured first mode natural frequency following Eq. (1) or Eq. (14), $(E_cI_0)_{iP\Delta}$ is the product of I_o/I_g and $(E_cI_g)_{P\Delta}$ which is the flexural rigidity computed by P-Δ relationship before cracking for PCB after grouting (bonded). Both values of $(E_cI_0)_{iACI}$ and $(E_cI_0)_{iP\Delta}$ are used for comparing reference. Since the properties of concrete materials are non-homogeneous and shall be affected by the several uncertain factors as manufacturing process, curing conditions, and distribution of micro-cracks etc. Hence $(E_cI_0)_{iACI}$ can not represent the actual initial flexural rigidities. As for $(E_cI_0)_{iP\Delta}$, these values derived from concrete beams had been prestressed don't match the definition of initial flexural rigidities for

Table 2. Comparison of initial flexural rigidities of PCB before prestressing computed by three approaches.

Specimen Designation	P-Δ test		$(E_cI_g)_{P\Delta}$ (KN-m^2)	Initial Flexural Rigidities (KN-m^2)		
	Pcr (KN)	δ (mm)		$(E_cI_0)_{iP\Delta}$	$(E_cI_0)_{i\omega}$	$(E_cI_0)_{iACI}$
P500	14.55	2.260	4,853	4,675	4887	8,274
P625	15.63	1.560	7,551	7,273	7658	8,274
P750	16.70	1.630	7,724	7,440	8687	8,274
S500	14.55	1.480	7,411	7,138	7300	8,227
S750	16.70	1.930	6,524	6,284	6154	8,227

Table 3. Variation of flexural rigidities for PCB prestressed before grouting (PCB with unbonded tendon).

Specimen Designation	Prestressing Force P_s (KN)	Before prestressing		Prestressed before grouting		$(EcI_0)_{iP\Delta}$ (KN-m^2)	$\varphi_{u1}=\frac{(E_cI_0)_{iP\Delta}}{(E_cI_0)_{p\omega}}$	$\varphi_{u2}=\frac{(E_cI_0)_{p\omega}}{(E_cI_0)_{i\omega}}$
		ω_{b1} (Hz)	$(E_cI_0)_{i\omega}$ (KN-m^2)	ω_{p1} (Hz)	$(E_cI_0)_{p\omega}$ (KN-m^2)			
P500	31.39	27.00	4,887	26.20	4,614	4,675	1.013	0.944
P625	39.24	33.80	7,658	32.00	6,888	7,273	1.056	0.899
P750	47.09	36.00	8,687	33.00	7,330	7,440	1.015	0.844
S500	31.39	33.00	7,300	33.00	7,300	7,138	0.978	1.000
S750	47.09	30.30	6,154	30.30	6,154	6,284	1.021	1.000

Table 4. Variation of flexural rigidities for PCB prestressed after grouting (PCB with bonded tendon).

Specimen Designation	Prestressing Force P_s (KN)	Before prestressing (KN-m^2)		After grouting $(E_cI_g)_{P\Delta}$ (KN-m^2)	$\varphi_{u2}=\frac{(E_cI_g)_{p\omega}}{(E_cI_g)_{i\omega}}$
		$(E_cI_0)_{i\omega}$	$(E_cI_g)_{i\omega}$		
P500	31.39	4,887	5,073	4,853	0.957
P625	39.24	7,658	7,951	7,551	0.950
P750	47.09	8,687	9,019	7,724	0.856
S500	31.39	7,300	7,579	7,411	0.978
S750	47.09	6,154	6,389	6,524	1.021

beams before prestressing. By comparing $(E_cI_0)_{i\omega}$ with those two reference values in Table 2, it shows values of $(E_cI_0)_{i\omega}$ are slightly greater and closed to the values of $(E_cI_0)_{iP\Delta}$, but far less than the values of $(E_cI_0)_{iACI}$. Based on this comparison, values of $(E_cI_0)_{i\omega}$ are relatively reasonable as initial flexural rigidities for the following discussion.

Table 3 shows the variation of flexural rigidities for PCB prestressed before grouting (simulating PCB with unbonded tendon). Comparing $(E_cI_0)_{p\omega}$ flexural rigidity computed by measured frequencies ω_{p1} following Eq. (22) with $(E_cI_0)_{iP\Delta}$, these two values are very closed just with 2~6% deviation (see column φ_{u1} in Table 3). This reveals that both ω_{p1} and Eq. (22) proposed in this study are consistent with each other and letting $(E_cI_0)_{p\omega}$ as flexural rigidities for PCB prestressed before grouting is a valid assumption. Then comparing ω_{b1},$(E_cI_0)_{i\omega}$ with ω_{p1}, $(E_cI_0)_{p\omega}$, it finds that natural frequencies (flexural rigidities) of PCB with parabolic unbonded tendons will decrease with increasing prestressing force. But natural frequencies (flexural rigidities) will not be affected by prestressing forces for PCB with straight unbonded tendons. As for predicting the amount of variation of natural frequency for PCB with unbonded tendon, Eq. (22) proposed previously is available.

Comparing $(E_cI_g)_{P\Delta}$ with $(E_cI_0)_{i\omega}$ for each specimen in Table 4, it reveals that $(E_cI_g)_{P\Delta}$ decrease with increasing prestressing force for PCB with parabolic bonded tendon similar to unbonded tendon as mentioned above. For PCB with straight bonded tendon, neglecting the deviation of ±2% shown in column φ_b in Table 4, flexural rigidities will also not be affected by prestressing forces as for unbonded tendon.

2. Effect Moment of Inertia for PCB

Comparing computed immediate deflection curve (black line) with testing load-deflection curve in Fig. 8, it reveals that computed deflection is always greater than testing deflection at the same loading. This results will over-optimistically assess the extent of cracking of PCB and lead to un-safety.

Following Notes on ACI 318-95 [8], both of c in Eq. (5) and I_{cr} in Eq. (6) are independent of prestressed forces, then all the I_{cr} of specimens are the same. It seem unreasonable for PCB. It is well known that prestressing forces may constrain and postpone the development of cracking, so the I_{cr} of PCB will greater than I_{cr} of reinforce concrete beam with the same amount of prestressing and non-prestressing steel but not prestressed. This study proposes force equilibrium method to compute c in Fig. 7 and use the same manner to calculate I_{cr} in Eq. (6).

Table 5. Moment of inertia of cracked section calculated by proposed method.

Specimen Designation	E_c (MPa)	f_c' (MPa)	f_{ps} (MPa)	$\Delta f_{ps} = f_{ps}$-f_{pe} (MPa)	c (cm)	I_{cr} (cm^4)
P500	13,481	8.23	521	114	-	36,000
P625	20,975	19.92	1188	680	14.19	22,475
P750	21,456	20.84	1209	599	13.62	21,459
S500	20,586	19.18	1170	764	14.66	23,480
S750	18,121	14.87	1029	419	18.29	35,636

Note: The compressive strength of concrete of P500 is too low to failure before steel yield and I_{cr} is taken as I_g.

$$0.85 f_c' \beta_1 b \times c = A_s f_y + A_{ps} f_{ps} \tag{23}$$

Where f_c' is concrete specified compressive strength of concrete, β_1 = 0.85 is factor relating depth of equivalent rectangular compressive stress block to neutral axis depth. f_y = 412 MPa is specified yield strength of reinforcement, and according to ACI 318M-08 [1] the stress in prestressing steel at nominal flexural strength f_{ps} which is expressed as Eq. (24)

$$f_{ps} = f_{pu}\left\{1-\frac{\gamma_p}{\beta_1}\left[\rho_p \frac{f_{pu}}{f_c'}+\frac{d}{d_p}(\omega-\omega'\right]\right\} \tag{24}$$

Where f_{pu} = 1,658 MPa is specified tensile strength of prestressing steel, factor of type of prestressing steel γ_p is taken as 0.55 for this study, $\rho_p = \frac{A_{ps}}{bd_p}$, tensile reinforcement index ω is taken as $\frac{A_s f_y}{bdf_c'}$, and compressive reinforcement index ω' is taken as $\frac{A_s' f_y}{bdf_c'} = 0$ in this study.

Substituting the calculating values of f_{ps} of Eq. (24) and c of Eq. (23) into Eq. (6), the proposed I_{cr} are tabulated as Table 5. The immediate deflection curve (red line) computed with E_c and the effective moment of inertia I_e which is obtained by substituting proposed I_{cr}. into Eq. (4) is also plotted together with testing load-deflection curve as shown in Fig. 8. It shows the red line is very closed to testing curve for every specimen.

V. CONCLUSSIONS

The findings from the testing program and theoretical analysis are summarized as follows:

1. No matter what post-tensioned PCB with bonded or unbonded tendons, natural frequencies (flexural rigidities) of PCB with parabolic tendons will decrease with increasing prestressing force. But natural frequencies (flexural rigidities) will not be affected by prestressing forces for PCB with straight tendons.
2. Comparing the analytic results with testing data, Rayleigh's method is proved to be a simple and useful method to calculate the first mode of natural frequencies for PCB. Similarly, for higher mode natural frequencies, Rayleigh-Ritz method which is an extension of Rayleigh's method may be an effective method.
3. Eq. (4) which moment of inertia of cracked section is computed following Notes on ACI 318-95 would over-estimate the non-linear immediate deflection of PCB. A force equilibrium method is introduced and the computed results are very closed to the testing results.

REFERENCES

1. ACI 318M-08, *Building Code Requirements for Structural Concrete (ACI 318M-08) and Commentary*, American Concrete Institute, Farmington Hills, MI, p. 289 (2008).
2. Breccolotti, M., Ubertini, F., and Venanzi, I., "Natural frequencies of prestressed concrete beams: theoretical prediction and numerical validation," *Proceeding of the XIX Aimeta Conference*, Ancona, Italy, pp. 14-17 (2009).
3. Dall'Asta, A. and Dezi, L., "Prestress force effect on vibration frequency of concrete bridges - Discussion," *Journal of Structural Engineering*, Vol. 122, No. 4, p. 458 (1996).
4. Dall'Asta, A. and Leoni, G., "Vibrations of beams prestressed by internal frictionless cables," *Journal of Sound and Vibration*, Vol. 222, pp. 1-18 (1999).
5. Deak, G., "Prestress force effect on vibration frequency of concrete bridges - Discussion," *Journal of Structural Engineering*, Vol. 122, No. 4, pp. 458-459 (1996).
6. Hamed, E. and Frostig, Y., "Natural frequencies of bonded and unbonded prestressed beams – prestress force effects," *Journal of Sound and Vibration*, Vol. 295, pp. 28-39 (2006).
7. Jain, S. K. and Geol, S. C., "Prestress force effect on vibration frequency of concrete bridges - Discussion," *Journal of Structural Engineering*, Vol. 122, No. 4, pp. 459-460 (1996).
8. Portland Cement Association, *Notes on ACI 318-95 Building Code Requirements For structural Concrete with Design Application*, 6th Edition, Illinois, pp. 8-2~8-6 (1996).
9. Raju, K. K. and Rao, G. V., "Free vibration behavior of prestressed beams," *Journal of Structural Engineering*, Vol. 112, No. 2, pp. 433-436 (1986).
10. Rao, S. S., *Mechanical Vibrations*, 5th Edition, Pearson, Taiwan, p. 734 (2011).
11. Saiidi, M., Douglas, B., and Feng, S., "Prestress force effect on vibration frequency of concrete bridges," *Journal of Structural Engineering*, Vol. 120, No. 7, pp. 2233-2241 (1994).
12. Thomson, W. T., *Theory of Vibration with Applications*, 5th Edition, Prentice Hall, New Jersey, pp. 281-285 (2001).